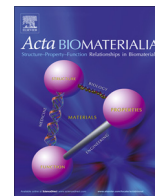


Contents lists available at [ScienceDirect](http://ScienceDirect.com)

Acta Biomaterialia

journal homepage: www.elsevier.com/locate/actabiomat

Supermacroporous chemically cross-linked poly(aspartic acid) hydrogels

Benjámín Gyarmati^a, E. Zsuzsanna Mészár^a, Lóránd Kiss^b, Mária A. Deli^b, Krisztina László^a, András Szilágyi^{a,*}^a Department of Physical Chemistry and Materials Science, Budapest University of Technology and Economics, Budafoki út 8., H-1111 Budapest, Hungary^b Institute of Biophysics, Biological Research Centre of the Hungarian Academy of Sciences, Temesvári krt. 62, H-6726 Szeged, Hungary

ARTICLE INFO

Article history:

Received 3 November 2014

Received in revised form 5 April 2015

Accepted 21 April 2015

Available online xxx

Keywords:

Poly(aspartic acid)

Hydrogel

Macroporous morphology

Responsive character

ABSTRACT

Chemically cross-linked poly(aspartic acid) (PASP) gels were prepared by a solid–liquid phase separation technique, cryogelation, to achieve a supermacroporous interconnected pore structure. The precursor polymer of PASP, polysuccinimide (PSI) was cross-linked below the freezing point of the solvent and the forming crystals acted as templates for the pores. Dimethyl sulfoxide was chosen as solvent instead of the more commonly used water. Thus larger temperatures could be utilized for the preparation and the drawback of increase in specific volume of water upon freezing could be eliminated. The morphology of the hydrogels was characterized by scanning electron microscopy and interconnectivity of the pores was proven by the small flow resistance of the gels. Compression tests also confirmed the interconnected porous structure and the complete re-swelling and shape recovery of the supermacroporous PASP hydrogels. The prepared hydrogels are of interest for several biomedical applications as scaffolding materials because of their cytocompatibility, controllable morphology and pH-responsive character.

© 2015 Acta Materialia Inc. Published by Elsevier Ltd. All rights reserved.

1. Introduction

Poly(aspartic acid) (PASP), a synthetic poly(amino acid), has gained remarkable attention recently for multiple reasons. PASP is biocompatible because of its chemical structure [1,2]. It is proved to be biodegradable, but its degradation rate depends on the type and degree of substitution [3]. Its precursor anhydride, polysuccinimide (PSI), reacts with primary amines under mild reaction conditions even without catalyst [1,4]. As PSI derivatives can be easily hydrolyzed to the corresponding PASP, a wide range of PASP derivatives can be synthesized including responsive PASP polymers and hydrogels [5–9]. All these benefits have initiated the fabrication of PASP-based biomedical devices both on macro and nanoscale [7–10]. Including aspartic acid repeating units makes possible the conjugation with *N*-terminated biomolecules via the carboxyl groups. The controllable ionic charge of this repeating unit was already utilized in the fabrication of biomimetic materials [11]. Nevertheless, the use of cross-linked PASP hydrogels has not yet been explored in tissue engineering, although several characteristics, e.g. large water uptake, externally controlled properties,

or soft characteristics, make PASP hydrogels suitable for applications in regenerative medicine.

In tissue engineering, damaged tissues or organs are replaced by implantation of cell cultures seeded on a biomaterial *in vitro*, or by implantation of scaffolds to promote the self-repair of the injured tissues [12]. Scaffolding materials must meet some basic requirements that are independent of the proposed application: they must be biocompatible and possess high porosity with a pore size suitable for the accommodation of the cells [13]. The pore size should be between 5 and 200 μm depending on the type of cell, and the pore structure in this specific size range is also referred to as supermacroporous morphology. A further requirement is the interconnectivity of pores to provide sufficient flow of the nutrient solution between the cells and the environment. The biomaterial must possess functional groups to enable facile modification of the surface with recognition sites, growth factors and ligands for control of the cell-scaffold interactions [12]. In addition, *in vitro* cell seeding and harvesting require easy control of cell adhesion and detachment by external stimulus (e.g. enzymatic treatment or temperature stimulus), while *in vivo* application of scaffolds demands controlled biodegradability of the biomaterial [14]. Finally, proper mechanical strength is also a general requirement towards scaffolding materials [15].

Thermally induced solid–liquid phase-separation during polymerization and/or cross-linking – also called cryogelation – is used to prepare porous structures. In the case of hydrogels, it

* Corresponding author. Tel.: +36 1 463 3518; fax: +36 1 463 3767.

E-mail addresses: gyarmati@mail.bme.hu (B. Gyarmati), meszar.ezsuzsa@gmail.com (E.Zs. Mészár), lorand.kiss.work@gmail.com (L. Kiss), deli@brc.hu (M.A. Deli), klaszlo@mail.bme.hu (K. László), aszilagyi@mail.bme.hu (A. Szilágyi).

is a well-established technique to create supermacroporous hydrogels below the melting point of the solvent [13]. The major part of the solvent is frozen during cryogelation, while the reaction occurs in the liquid phase, which is a concentrated solution of the polymer [16,17]. The growing crystals of the solvent act as templates for the interconnected pores forming after melting. Here we report the synthesis of supermacroporous PASP hydrogels by cryogelation in DMSO. Additionally the pore morphology, pore interconnectivity and mechanical properties of prepared hydrogels were investigated.

2. Experimental section

2.1. Materials

1,4-diaminobutane (DAB, 99%), imidazole (puriss) and 2,4,6-trinitrobenzenesulfonic acid (picrylsulfonic acid, TNBS, 1 M aqueous solution, analytical reagent) were obtained from Sigma-Aldrich. Dimethyl sulfoxide (DMSO, dried, max. 0.025% H₂O), L-aspartic acid (99%), methanol (MeOH, 99.9%), potassium chloride (99.5%), sodium tetraborate decahydrate (a.r.), mesitylene (for synthesis) and sulfolane (for synthesis) were acquired from Merck. Phosphoric acid (cc. 85%) and hydrochloric acid (HCl, 35%) were purchased from Lach Ner. Citric acid monohydrate (99%) and sodium hydroxide (NaOH, a.r.) were bought from Reanal (Hungary). For cytotoxicity tests Eagle's minimum essential medium (MEM; Gibco), fetal bovine serum (Lonza), Na-pyruvate (Gibco), XTT (2,3-bis(2-methoxy-4-nitro-5-sulphophenyl)-2H-tetrazolium-5-carboxanilide inner salt, Roche) and cytotoxicity detection kit measuring LDH (lactate dehydrogenase) release (Roche), 96-well and 24-well cell culture plates (Orange, UK) were used. All reagents and solvents were used without further purification.

The aqueous buffer solutions used were prepared from citric acid ($c = 0.033$ M, pH = 2 to 6), imidazole ($c = 0.1$ M, pH = 6 to 8) and sodium tetraborate ($c = 0.025$ M, pH = 8 to 12). pH was adjusted by the addition of 1 M HCl or 1 M NaOH. Ionic strength of the solutions was adjusted to 0.15 M by the addition of KCl. The pH of the buffer solutions was checked with a pH/ion analyzer (Radelkis OP-271/1).

2.2. Methods

2.2.1. Synthesis

The PSI polymer was synthesized by the acid-catalysed thermal polycondensation of aspartic acid in a mixture of mesitylene and

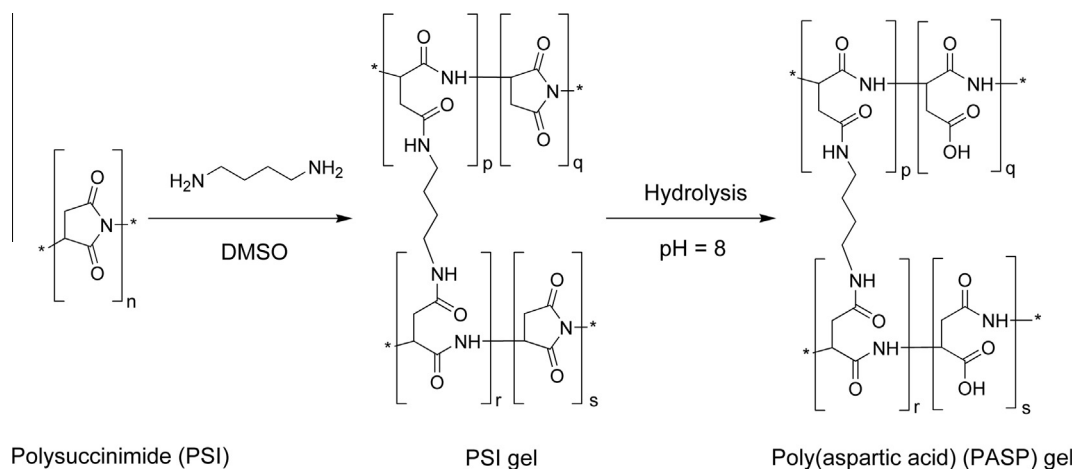
sulfolane at 160 °C (7 h) [8]. PSI was purified by precipitation in methanol and dried in vacuum at 25 °C. Its chemical structure was confirmed by ¹H NMR (300 MHz, DMSO-d₆, δ): 5.10 (d, 1H, CH); 3.20 and 2.75 (s,s, 2H, CH₂). After hydrolysis the average molecular weight of the resultant PASP was determined by HPLC size exclusion chromatography (SEC). A Nucleogel GFC-300 (Macherey–Nagel) column was used (molecular mass range 1–100 kDa) with phosphate buffered saline (PBS, pH = 7.6) eluent. The average molecular mass of PASP was 56.1 kDa with polydispersity index of 1.07.

PSI was cross-linked with 1,4-diaminobutane under cryogenic conditions in DMSO significantly below the melting temperature (−10 to −40 °C) to induce phase separation (Scheme 1). In a typical procedure of gel synthesis, the solution of the cross-linker (8.8 wt.% DAB in DMSO) was added to the solution of PSI (final concentration of 9.70 wt.% in DMSO). The cross-linking ratio (X_{DAB} defined as the molar ratio of cross-linker molecules to the repeat units) in the precursor solution varied between 4.0% and 9.0%. After 30 s vigorous stirring at 25 °C the precursor solution was filled into the sample holders and quickly placed in a freezer. For the swelling experiments and SEM measurements gel sheets with thickness of 2 mm were prepared, while for the mechanical characterization and flow experiments samples were prepared in cylindrical molds (diameter ≈ height ≈ 1.5 cm). The temperature was continuously controlled (deviation less than ±2 °C). After 7 days gelation time, the sample holders containing PSI-DAB gels were quickly immersed into room temperature aqueous buffer solution (pH = 8) to yield the PASP-DAB gels.

2.2.2. Characterization

The conversion of the cross-linking reaction was characterized by the number of unreacted cross-linker molecules, which is determined by a method developed earlier [18]. After cryogelation, the swelling solution of PSI-DAB gels were reacted with TNBS at pH = 9. The concentration of unreacted cross-linker molecules, and hence the conversion, was determined by the UV–Vis spectrophotometric assay of the TNBS adduct of DAB (details in Supplementary Data).

Cytotoxicity and viability tests were made on human intestinal epithelial Caco-2 cells [19]. The PBS solutions in which the PASP hydrogels were swollen during sterilization were used in the biological tests. The negative control group received culture medium diluted with PBS while the positive control group was treated with 1% Triton X-100 detergent. Viability was determined by measuring the cellular conversion of XTT dye, whereas cytotoxicity was



Scheme 1. Synthesis of PSI and PASP gels. Additional cross-linking in water is prohibited after cryogelation of PSI.

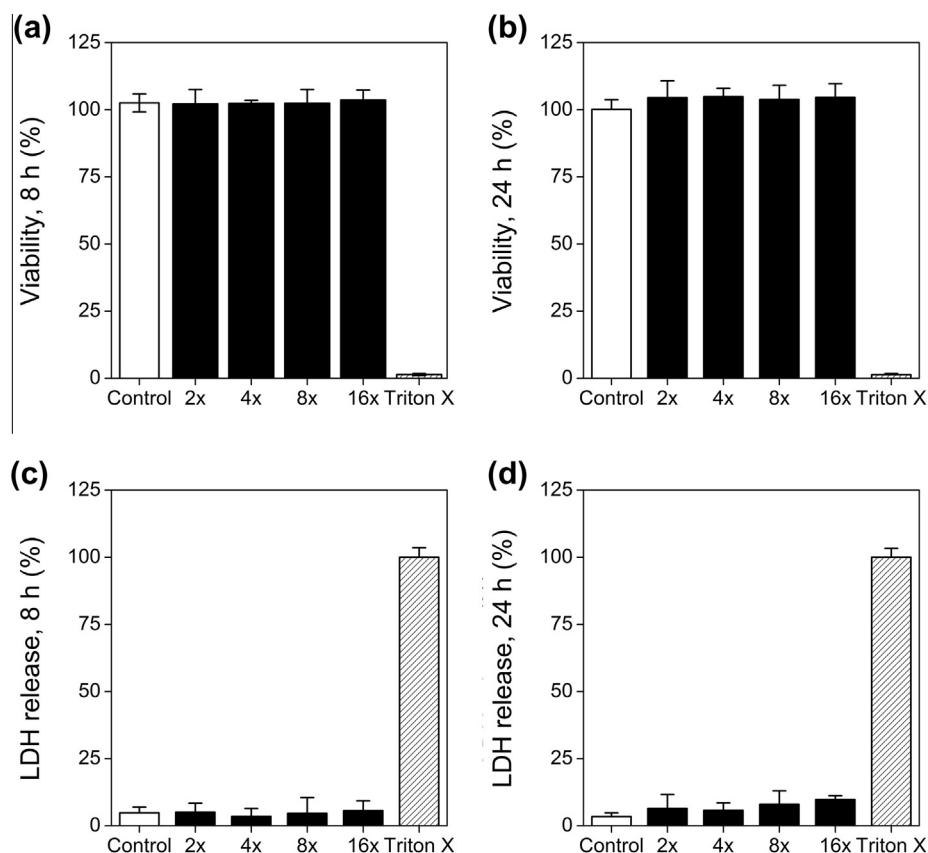


Fig. 1. Cellular viability after (a) 8 h and (b) 24 h and cytotoxicity after (c) 8 h and (d) 24 h treatment of human epithelial cells with PBS solution in which the PASP hydrogels were sterilized.

Table 1
Characteristic pore sizes and their aspect ratio in supermacroporous PASP hydrogels.

T_{gel}^a (°C)	X_{DAB}^b (%)	Shortest size (μm)	Longest size (μm)	Aspect ratio (-)
-30	6	66 ± 19	259 ± 193	4.0 ± 2.9
-30	7	12 ± 5	25 ± 17	2.1 ± 1.2
-10	6	17 ± 12	25 ± 17	1.6 ± 0.5
-10	7	9 ± 4	11 ± 4	1.3 ± 0.2

^a Gelation temperature.

^b Molar ratio of 1,4-diaminobutane to the repeating units of polymer.

characterized by the LDH release of the cells after predetermined time intervals (details in [Supplementary Data](#)).

The morphology of PASP gels was characterized by scanning electron microscopy (SEM, JEOL JSM 6380 LA, accelerating voltage 15 kV). To preserve their porous structure, after dialysis in water, the hydrogels were dropped into liquid nitrogen and freeze-dried prior to SEM imaging. Solid specimens were coated with gold. Micrographs were always taken from the bulk material to avoid edge effects. Two characteristic pore sizes (longest and shortest) were determined for each gel from the micrographs and the aspect ratio of the pores was calculated.

The permeability of the PASP-DAB gels was tested by flow resistance model experiments. A cylindrical sample was put into a plastic syringe with an inner diameter of 10 mm. The flow rate of a buffer solution (pH = 8) passing through the hydrogel was controlled by changing the height of the reservoir containing the buffer solution. The lower and the upper limits of the hydrostatic pressure were determined by the geometric barrier of the reservoir.

The pH-dependent response of PASP-DAB hydrogels was determined by swelling experiments. PASP-DAB hydrogel discs of diameter $d_0 = 10$ mm were cut from the gel sheets (equilibrated at pH = 8, ambient temperature) and transferred into buffer solutions of various pH values ranging from 2 to 12 for 12 h. The degree of swelling was defined as the ratio of the diameter d of the gel at the given pH to the initial diameter d_0 .

The mechanical properties of the PASP-DAB hydrogels were characterized with uniaxial compression tests using an Instron 5543 mechanical tester with cell load of 5 N. The force (F) and the extent of compression (Δh) of the cylindrical samples were recorded during the measurements, and the nominal stress (σ_n) and strain (ε) were calculated using the following equations: $\sigma_n = F/A_0$ and $\varepsilon = \Delta h / h_0$, where A_0 is the cross-sectional area of the undeformed hydrogel and h_0 is the original height. The maximum strain ε did not exceed 30%. The compression tests consisted of three main steps. A continuous compression with a constant deformation rate was applied in the first step, followed by 10 s relaxation. Deformation was decreased to zero with the same deformation rate as in the first step. Moduli were determined from the linear fit to the stress-strain function between 0% and 10% strain (in the direction of increasing strain).

2.2.3. Statistical analysis

Cellular viability, toxicity, the pore size of the gels and flow rate data are expressed as the mean \pm standard error using Student's t-test with a significance level of $p < 0.05$. The statistical difference of pore sizes and degree of swelling were analyzed by the unpaired t-test ($p < 0.05$).

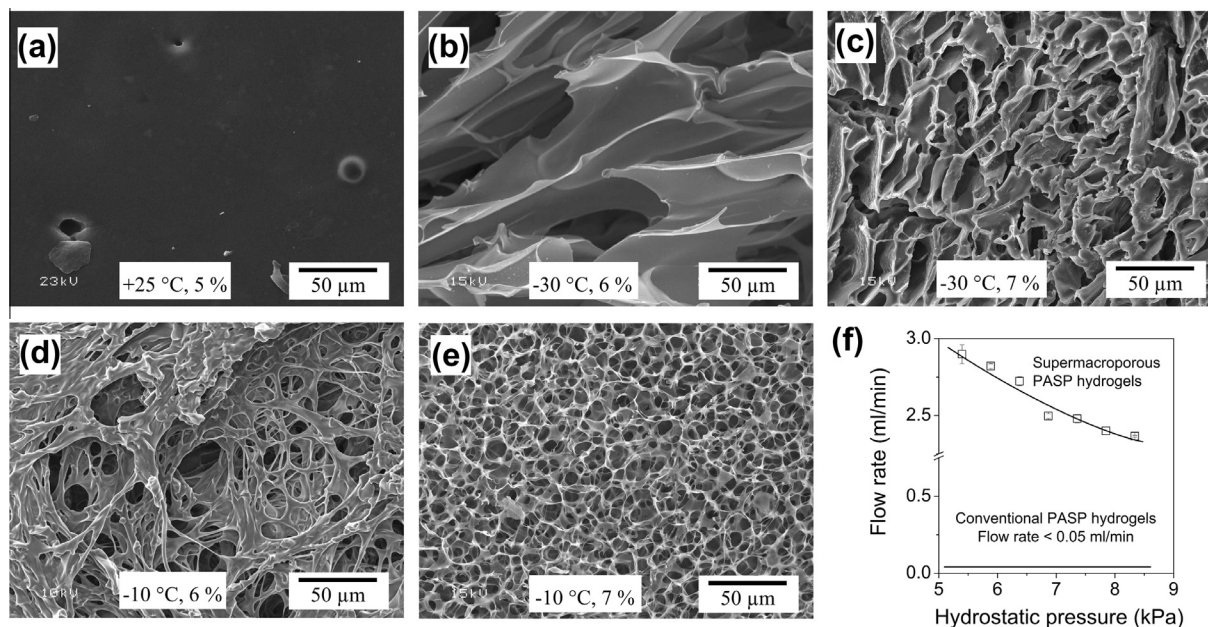


Fig. 2. (a)–(e) SEM micrographs of PASP gels (T_{gel} and X_{DAB} are indicated in each micrograph), (f) flow rate of the swelling agent through supermacroporous ($T_{\text{gel}} = -20$ °C, $X_{\text{DAB}} = 5\%$) and conventional PASP hydrogels ($T_{\text{gel}} = 25$ °C, $X_{\text{DAB}} = 5\%$) as a function of hydrostatic pressure.

3. Results and discussion

Water-swellaable macroporous PASP hydrogels was synthesized by cross-linking PSI with DAB below the freezing point of DMSO and the subsequent hydrolysis of PSI gels. The high reactivity of succinimide rings of the polymer and the amine groups of the cross-linker molecules results in high conversion. In PASP gels prepared at room temperature the molar ratio of unreacted amines compared to their feed amount is negligible (smaller than 1%) after the cross-linking reaction [5,18]. Nonetheless, the decreased temperature of cryogelation might significantly affect the reactivity, so we employed an analytical method using TNBS to determine the conversion of the cross-linker molecules during cryogelation. We observed that a measurable amount of cross-linker molecules remained unreacted, but below 2% independently of the cross-linking ratio. Consequently, the cross-linking density is smaller in gels prepared by cryogelation, but we can expect sufficient chemical stability from the cryogels because of the high conversion values. The reduced reactivity at low temperatures is indicated by the dissolution of cryogels at pH = 8 obtained after 1 day reaction time. A gelation time of 7 days was therefore chosen to prepare cryogels that were stable over several weeks at pH = 8.

The biocompatibility of PASP hydrogels is a prerequisite for any future application as surfaces or scaffolds for cell seeding and proliferation. Accordingly, the cytotoxicity of PASP matrices was investigated by XTT and LDH tests [7,19]. The negative control, which consisted of the culture medium diluted two-fold with sterile PBS, showed 100% cellular viability (Fig. 1(a) and (b)) and practically 0% cellular toxicity (Fig. 1(c) and (d)). Cells treated with Triton X-100, the positive control for cellular toxicity, were killed in all tests (indicated by the low viability in Fig. 1(a) and (b) and by the large LDH release in Fig. 1(c) and (d)). PASP hydrogels showed similar values to negative control groups in both the LDH release and XTT assays ($p < 0.05$) after both 8 and 24 h. These results indicate that no compounds that are toxic to cultured human cells were released from PASP gels, which lends support to biological applications of the hydrogels.

Controlled pore structure of PASP hydrogels was achieved by using cryogelation. Although water is the most frequently used

solvent in cryogelation, this time DMSO was used for the preparation of the macroporous gels for several reasons. The thermal expansion of DMSO upon freezing is considerably smaller than that of water. Also, the freezing point of DMSO is higher (19 °C), and therefore the phase separation can be induced already at higher temperature than in water. PSI can be readily cross-linked in DMSO without any catalyst contrary to water, which is a poor solvent of the precursor polymer. DMSO is miscible in water, and for this reason unreacted chemicals and the solvent could be easily removed by aqueous buffer solution (pH = 8). Since water is a poor solvent of PSI, additional cross-linking of PSI after cryogelation is hindered at room temperature and the hydrolysis results in PASP gels with the same cross-linking ratio as PSI gels (Scheme 1). A minimal cross-linking ratio of 4% was necessary to prevent dissolution of the gels during hydrolysis. Thus hydrogels with $X_{\text{DAB}} = 4$ to 9% were used in further experiments. As a comparison, PSI gels were prepared also at room temperature (gelation temperature, $T_{\text{gel}} = 25$ °C) and hydrolyzed to PASP gels, subsequently referred to as conventional PASP hydrogels. Contrary to the conventional PASP hydrogels, cryogelation of PSI resulted in supermacroporous PASP hydrogels (representative examples are shown in Fig. 2(a)–(e)). Both cross-linking ratio and gelation temperature affect the morphology of the hydrogels (pore sizes are statistically different as a function of T_{gel} and X_{DAB} , $p < 0.05$). It is clearly demonstrated that lower gelation temperature and decreasing cross-linking ratio result in larger pore sizes (Table 1).

Temperature plays a crucial role in the cryogelation process. It must be far below the freezing point of the pure solvent, partly because of the freezing point depression in the presence of solutes, partly because of the overcooling phenomenon, i.e., the solvent may be in a metastable state directly below its freezing point. The uncertain temperature profile during overcooling and freezing results in poor control of the cryogelation process. As Fig. 2 shows, porous morphology was observed even at -10 °C in DMSO, which is not sufficiently low to prepare cryogels in aqueous medium [20]. Thus, in practice, we have a wider temperature range to prepare cryogels in DMSO than in water, which may provide better control over morphology and make available a wider range of pore sizes. Lower gelation temperatures resulted in larger pores (Table 1), in

agreement with Okay et al. [21]. The explanation is based on the thermodynamic interpretation of solid–liquid phase separation. Lower temperatures yield larger crystals and a more limited reaction zone, which leads to formation of larger pores. The relatively large aspect ratio at the lower temperature ($-30\text{ }^{\circ}\text{C}$) (Table 1) indicates the alignment of the pore structure (especially in Fig. 2(b)). This internal “ladder-like” structure is a result of local temperature gradients that develop during cryogelation. Elevated temperatures ($-10\text{ }^{\circ}\text{C}$) favor a random pore structure with aspect ratio close to 1.

Feed composition also affects the morphology of the gels. Larger cross-linking ratios accelerate gelation, and the formation of the chemical network can hinder the crystal growth of the solvent, resulting in smaller average pore sizes (Table 1). Thus, the average pore size is controlled by the reaction kinetics, which is also influenced by the temperature.

The interconnectivity of the pores was investigated by flow-through measurements. The considerable flow rate measured through supermacroporous PASP hydrogels (Fig. 2(f)) confirmed the convective transport, and hence the interconnectivity of the pores. Nevertheless, the flow rate decreases with increasing hydrostatic pressure, in apparent contradiction to intuitive expectation. However, the pores deform under load, and as a result some flow channels even may become totally blocked inside the gel. As a comparison, the flow rate through conventional PASP hydrogels is also shown (Fig. 2(f)). The buffer solution practically cannot flow through the conventional PASP gels because the fluid transport is diffusion-controlled.

The degree of swelling of the conventional PASP hydrogels can be controlled by the pH, owing to dissociation of the aspartic acid repeating units above the pK_a of the polymer [8]. Supermacroporous PASP hydrogels are also expected to exhibit pH-dependent swelling. Preliminary experiments showed that the effect of the gelation temperature on the degree of swelling is negligible, suggesting that the temperature does not strongly influence the final composition of the network. Consequently, the effect of cross-linking ratio on pH-dependent swelling is well defined (Fig. 3). The pH-dependence at cross-linking ratio larger than 7% is not significant (not shown). The pH-dependence of degree swelling of the supermacroporous hydrogels showed a similar tendency as conventional PASP gels (Fig. 3). The degree of swelling increases significantly in the pH range 3–5 in both cases. The relative increase in degree of swelling upon increasing pH is slightly smaller at larger cross-linking ratio (the difference of the curves at acidic pH values is confirmed by the unpaired t-tests of the degree of swelling at $\text{pH} = 2.5$ ($p < 0.05$)) because of the larger number of chemical cross-links per unit volume of gel. The influence of pH is more pronounced in the case of supermacroporous gels. This may be explained by the smaller concentration of chemical junction points in supermacroporous hydrogels because of the lower conversion of cross-linking molecules at the gelation temperature.

The mechanical properties of PASP hydrogels were investigated for the gelation temperatures -20 and $-10\text{ }^{\circ}\text{C}$ because lower values of T_{gel} resulted in poorly defined pore structures (Fig. 2). PASP hydrogels prepared at $-10\text{ }^{\circ}\text{C}$ could not withstand deformations as large as 20%, in contrast to the large deformability of gels prepared at $-20\text{ }^{\circ}\text{C}$. Accordingly, the uniaxial compression modulus measurements were made on these gels and the moduli are listed in Table 2. The prepared hydrogels are very soft matrices with compression modulus between 0.1 and 1 kPa, which is relatively small and can be explained by the lower conversion of cross-linker molecules under cryogenic conditions. The gels with 4% cross-linking ratio are strongly deformed even under their own weight, which determines the lower limit of the cross-linking ratio. The gels with 9% cross-linking ratio did not display the sponge-like behavior, suggesting absence of the interconnected

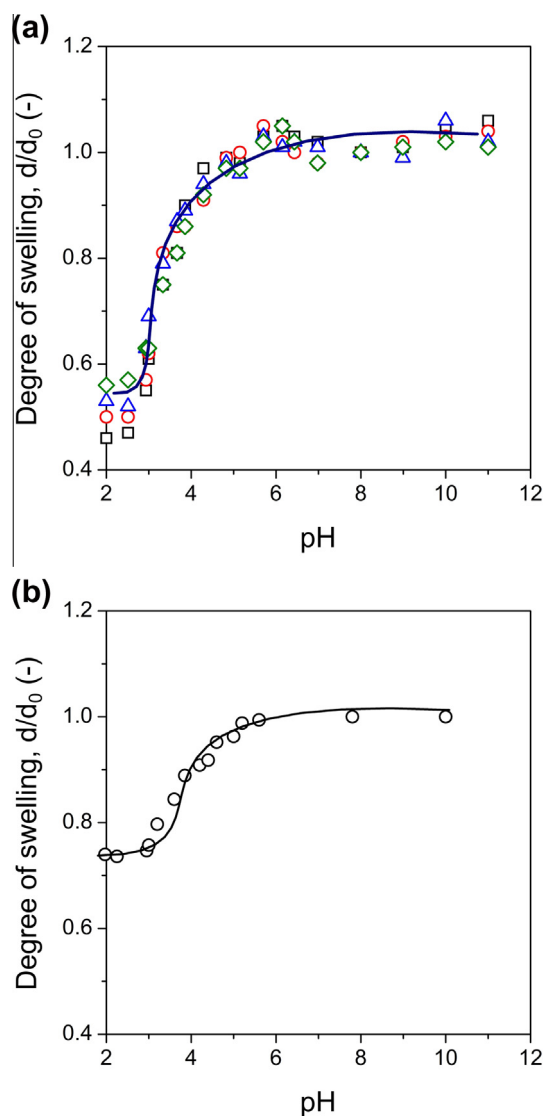


Fig. 3. (a) pH-dependent swelling of supermacroporous PASP hydrogels at ambient temperature. $T_{\text{gel}} = -20\text{ }^{\circ}\text{C}$, X_{DAB} : \square 4%, \circ 5%, \triangle 6%, \diamond 7% (b) pH-dependent swelling of conventional PASP hydrogels. Curves are to guide the eye. The reference diameter (d_0) is measured at $\text{pH} = 8$. The standard error of the swelling data of macroporous gels was determined at $\text{pH} = 2.5$ (2.1%, $p < 0.05$) and at $\text{pH} = 6.5$ (3.4%, $p < 0.05$).

Table 2

Compression modulus of macroporous PASP hydrogels as a function of cross-linking ratio ($T_{\text{gel}} = -20\text{ }^{\circ}\text{C}$).

X_{DAB} (-)	Compression modulus (Pa)
5	110 \pm 1
7	224 \pm 10
9	740 \pm 13

pore structure. $X_{\text{DAB}} = 5\%$ was chosen because of the excellent reproducibility of the properties of these gels, including small variation of the modulus. The deformability of these gels was always above 25% for several cycles. Larger cross-linking ratios resulted in fracture of the gel under a deformation of 20% after a few deformation cycles.

As we have seen, supermacroporous PASP hydrogels with properly chosen cross-linking ratio can be compressed without mechanical destruction and they generally recover their original shape after the compression [22]. A cylindrical conventional PASP

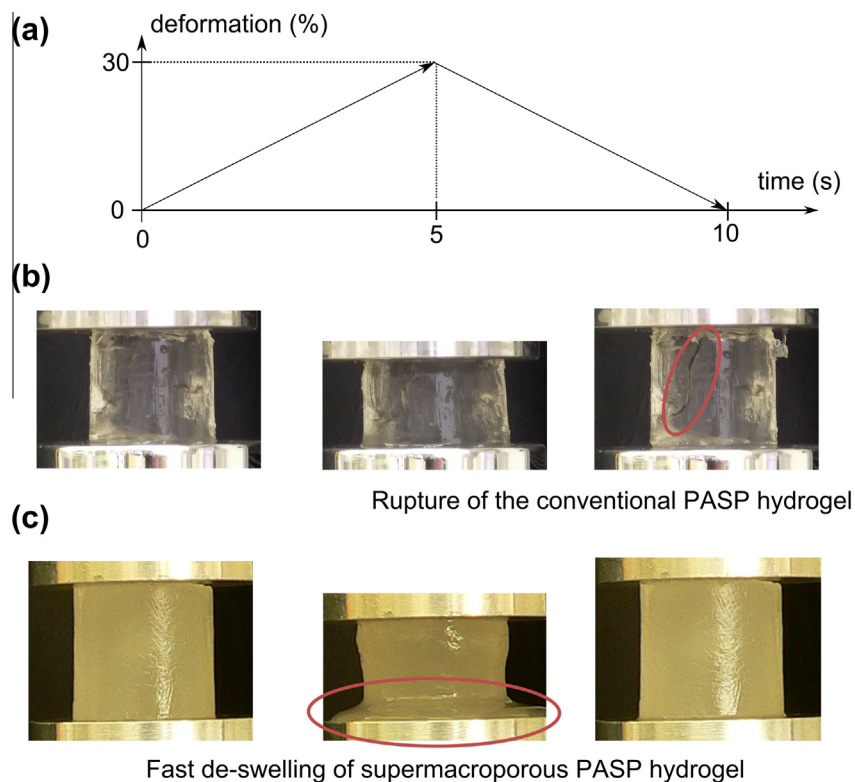


Fig. 4. (a) Measurement profile of the mechanical test applied for the comparison of conventional and supermacroporous PASP hydrogels; (b) rupture of the conventional gel ($T_{\text{gel}} = 25\text{ }^{\circ}\text{C}$, $X_{\text{DAB}} = 5\%$) upon compression to 30% strain; (c) the supermacroporous PASP hydrogel ($T_{\text{gel}} = -20\text{ }^{\circ}\text{C}$, $X_{\text{DAB}} = 5\%$) recovers its initial shape.

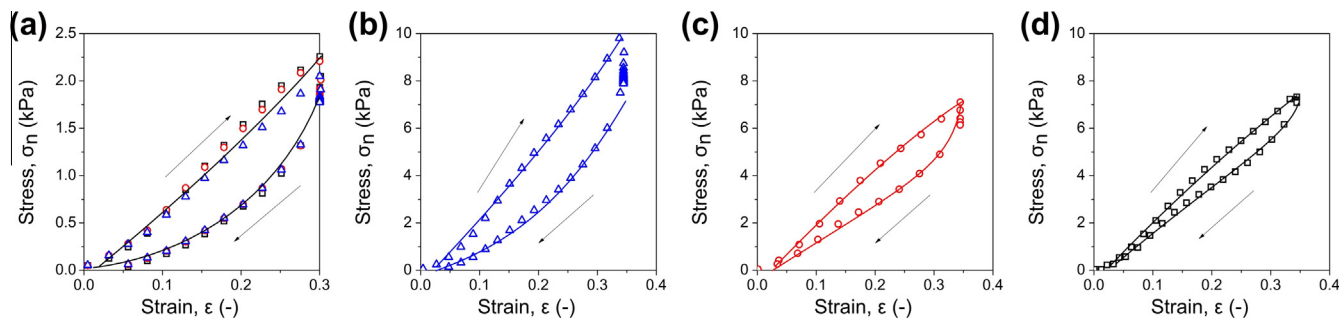


Fig. 5. Stress vs. strain curves of supermacroporous PASP hydrogels under cyclic mechanical load (a) at deformation rate 0.1 mm/s, \circ 1st run, \square 2nd run, \triangle 3rd run; ($T_{\text{gel}} = -20\text{ }^{\circ}\text{C}$, $X_{\text{DAB}} = 5\%$); at different deformation rates: (b) 1.0 mm/s, (c) 0.2 mm/s, (d) 0.1 mm/s ($T_{\text{gel}} = -20\text{ }^{\circ}\text{C}$, $X_{\text{DAB}} = 9\%$). For greater visibility, every 20th data point is shown in (b)–(d).

and a supermacroporous hydrogel sample were compared in a cyclic mechanical test, in which they were compressed to a relative deformation of 30% within 5 s and the load was released in the subsequent 5 s (test profile is shown in Fig. 4(a)). As Fig. 4(b) shows, the conventional PASP gel did not withstand the large deformation and a crack developed in the specimen. However, the supermacroporous PASP hydrogel recovered its original shape without cracks. Furthermore, the swelling agent of the gel is squeezed out upon compression, confirming the interconnectivity of the pores. As the load is released, the hydrogel reaches its initial degree of swelling in contact with its swelling agent. The observed sponge-like behavior cannot be properly characterized by conventional unidirectional compression tests [22]. We used a 3-step compressive test to model the dynamic loading of the hydrogels in a continuously changing biological environment. The stress was recorded both with increasing and decreasing strain.

A representative stress vs. strain curve is shown in Fig. 5(a). The supermacroporous hydrogels can be compressed without destruction and the gel recovers its original shape after the load was released. The curves corresponding to increasing and decreasing strain do not overlap. This type of hysteresis is often observed for highly stretchable or tough gels and explained by the energy-dissipation inside the network under stress [23]. The reason for this phenomenon is different in our case and can be explained by the concurring processes of swelling and deformation. A part of the swelling agent released upon compression cannot be taken up by the hydrogel if the rate of expansion is fast. The effect of rate of deformation on mechanical behavior is shown in Fig. 5(b)–(d). The cross-linking ratio was 9%, because the gels with lower cross-linking ratio could not withstand large deformation rates without mechanical destruction. We observed that both the stress and the size of the hysteresis loop significantly decrease with

slower deformation rate because the hydrogel approaches its equilibrium degree of swelling during compression.

Results of the compression tests indicate the stress relaxation of the supermacroporous PASP hydrogels with swelling and de-swelling processes due to the interconnected pore structure. However, the supermacroporous PASP hydrogels prepared were very soft, as shown by the low maximum stress upon compression. The compressive modulus of soft tissues is 0.4–350 MPa [24]. *In vivo* application of hydrogels demand similar moduli, otherwise any deformation ruptures the biomaterial. Consequently, reinforced supermacroporous PASP hydrogels have to be developed for future *in vivo* applications.

4. Conclusion

In conclusion, supermacroporous, chemically cross-linked poly(aspartic acid) (PASP) hydrogels were synthesized by cryogelation. DMSO was employed as the solvent instead of the more commonly used water, because DMSO has several substantial benefits such as higher gelation temperature, a smaller thermal expansion upon freezing, and the simple synthetic pathway. The pore sizes of the resultant PASP hydrogels were in the supermacroporous range and could be controlled by the gelation temperature and the cross-linking ratio. Interconnectivity of the pores was confirmed by small flow resistance. Compression tests indicated that, upon compression, the hydrogels released part of their swelling solution, which was taken up again upon release of the load. The supermacroporous PASP hydrogels displayed pH-responsive swelling similarly to the conventional PASP hydrogels. Results indicate that the hydrogels developed can be suitable for *in vitro* cell seeding with pH-induced detachment of the grown cells. The easy modification of the precursor polymer and the cytocompatibility of the PASP hydrogels argue in favor of the feasibility of future biological applications.

Acknowledgments

This research was supported by the OTKA Foundation (PD76401, K101861) and by the New Széchenyi Plan (TÁMOP-4.2.1/B-09/1-2010-0002). The financial support of FP-7 Marie Curie IRSES (ENSOR, project ID 269267) is acknowledged. András Szilágyi is grateful for the support of the János Bolyai Research Scholarship from the Hungarian Academy of Sciences.

Appendix A. Figures with essential colour discrimination

Certain figures in this article, particularly Figs. 3–5, are difficult to interpret in black and white. The full colour images can be found in the on-line version, at <http://dx.doi.org/10.1016/j.actbio.2015.04.033>.

Appendix B. Supplementary data

Supplementary data associated with this article can be found, in the online version, at <http://dx.doi.org/10.1016/j.actbio.2015.04.033>.

References

- [1] Joentgen W, Müller N, Mitschker A, Schmidt H. Polyaspartic acids. Biopolymers online. Wiley-VCH Verlag GmbH & Co. KGaA; 2005.
- [2] Roweton S, Huang SJ, Swift G. Poly(aspartic acid): synthesis, biodegradation, and current applications. *J Environ Polym Degr* 1997;5:175–81.
- [3] Lu Y, Chau M, Boyle AJ, Liu P, Niehoff A, Weinrich D, et al. Effect of pendant group structure on the hydrolytic stability of polyaspartamide polymers under physiological conditions. *Biomacromolecules* 2012;13:1296–306.
- [4] Torma V, Gyenes T, Szakács Z, Noszál B, Némethy Á, Zrínyi M. Novel amino acid-based polymers for pharmaceutical applications. *Polym Bull* 2007;59:311–8.
- [5] Gyenes T, Torma V, Gyarmati B, Zrínyi M. Synthesis and swelling properties of novel pH-sensitive poly(aspartic acid) gels. *Acta Biomater* 2008;4:733–44.
- [6] Zrínyi M, Gyenes T, Juriga D, Kim JH. Volume change of double cross-linked poly(aspartic acid) hydrogels induced by cleavage of one of the crosslinks. *Acta Biomater* 2013;9:5122–31.
- [7] Némethy Á, Solti K, Kiss L, Gyarmati B, Deli MA, Csányi E, et al. pH- and temperature-responsive poly(aspartic acid)-*l*-poly(N-isopropylacrylamide) conetwork hydrogel. *Eur Polym J* 2013;49:2392–403.
- [8] Gyarmati B, Vajna B, Némethy Á, László K, Szilágyi A. Redox- and pH-responsive cysteamine-modified poly(aspartic acid) showing a reversible sol-gel transition. *Macromol Biosci* 2013;13:633–40.
- [9] Tachibana Y, Kurisawa M, Uyama H, Kakuchi T, Kobayashi S. Biodegradable thermoresponsive poly(amino acids). *Chem Commun* 2003:106–7.
- [10] Zheng C, Zhang XG, Sun L, Zhang ZP, Li CX. Biodegradable and redox-responsive chitosan/poly(*l*-aspartic acid) submicron capsules for transmucosal delivery of proteins and peptides. *J Mater Sci: Mater Med* 2013;24:931–9.
- [11] Knight DK, Gillies ER, Mequanint K. Biomimetic *l*-aspartic acid-derived functional poly(ester amide)s for vascular tissue engineering. *Acta Biomater* 2014;10:3484–96.
- [12] Ma PX, Elisseeff J. Scaffolding in tissue engineering. New York: CRC Press, Taylor & Francis Group; 2006.
- [13] Mattiasson B, Kumar A, Galaev IY. Macroporous polymers: production properties and biotechnological/biomedical applications. New York: CRC Press, Taylor & Francis Group; 2010.
- [14] Dou X-Q, Yang X-M, Li P, Zhang Z-G, Schonherr H, Zhang D, et al. Novel pH responsive hydrogels for controlled cell adhesion and triggered surface detachment. *Soft Matter* 2012;8:9539–44.
- [15] Hutmacher D. Scaffold design and fabrication technologies for engineering tissues—state of the art and future perspectives. *J Biomater Sci Polym Ed* 2001;12:107–24.
- [16] Savina IN, Gun'ko VM, Turov VV, Dainiak M, Phillips GJ, Galaev IY, et al. Porous structure and water state in cross-linked polymer and protein cryo-hydrogels. *Soft Matter* 2011;7:4276–83.
- [17] Plieva FM, Galaev IY, Mattiasson B. Macroporous gels prepared at subzero temperatures as novel materials for chromatography of particulate-containing fluids and cell culture applications. *J Sep Sci* 2007;30:1657–71.
- [18] Gyarmati B, Hegyesi N, Pukánszky B, Szilágyi A. A colorimetric method for the determination of the degree of chemical cross-linking in aspartic acid-based polymer gels. *eXPRESS Polym Lett* 2015;9:154–64.
- [19] Kiss L, Walter FR, Bocsik A, Veszella S, Ózsvári B, Puskás LG, et al. Kinetic analysis of the toxicity of pharmaceutical excipients cremophor EL and RH40 on endothelial and epithelial cells. *J Pharm Sci* 2013;102:1173–81.
- [20] Plieva F, Huiting X, Galaev IY, Bergenstahl B, Mattiasson B. Macroporous elastic polyacrylamide gels prepared at subzero temperatures: control of porous structure. *J Mater Chem* 2006;16:4065–73.
- [21] Ozmen MM, Okay O. Superfast responsive ionic hydrogels with controllable pore size. *Polymer* 2005;46:8119–27.
- [22] Savina IN, Cnude V, D'Hollander S, Van Hoorebeke L, Mattiasson B, Galaev IY, et al. Cryogels from poly(2-hydroxyethyl methacrylate): macroporous, interconnected materials with potential as cell scaffolds. *Soft Matter* 2007;3:1176–84.
- [23] Sun J-Y, Zhao X, Illeperuma WRK, Chaudhuri O, Oh KH, Mooney DJ, et al. Highly stretchable and tough hydrogels. *Nature* 2012;489:133–6.
- [24] Hollister SJ. Porous scaffold design for tissue engineering. *Nat Mater* 2005;4:518–24.